Indoor RF signal distribution using a coherence multiplexed/subcarrier multiplexed optical transmission system

Robert Taniman, Arjan Meijerink*, Wim van Etten and Jaap Haartsen
University of Twente, Department of Electrical Engineering, Telecommunication Engineering Group
P.O. Box 217, 7500 AE, Enschede, The Netherlands
Email: a.meijerink@ieee.org

***Abstract*— A Radio over Fiber (RoF) distribution network based on single-mode fiber (SMF) and a combination of coherence multiplexing (CM) and subcarrier multiplexing (SCM) is proposed. CM is a relatively unknown and potentially inexpensive form of photonic code-division multiplexing, and is used here as a means to distinguish between the radio access points (RAPs). Two alternative CM network topologies are considered: one for downlink and one for uplink. SCM is used on top of CM in order to serve multiple users through the same RAP simultaneously. The performance of the system is analyzed, incorporating the effect of chromatic fiber dispersion, optical beat interference noise between the CM channels, shot noise, thermal noise and intermodulation distortion (IMD) between the SCM channels.**

I. Introduction

The growing interests in broadband wireless access give impetus to the development of Radio over Fiber (RoF) techniques [1], [2]. The RoF basic concept is to distribute the radio-frequency (RF) signals by optical transmission to radio access points (RAPs) so that the RAPs are not required to perform complicated functionalities such as modulation, coding, up/down conversion and multiplexing. These functionalities can then be concentrated in a central node, acting as a remote base station. This way, the RAPs can be made simpler, hence reducing the overall system's costs. In Figure 1, a simple example of an (indoor) RoF distribution network is shown.

In the proposed system, single-mode fiber (SMF) is used as a transmission medium, since multimode fiber and copper cables simply do not offer the required bandwidth to transport RF signals over typical indoor distances.

Coherence multiplexing (CM) [2]–[6] is proposed as a means to distinguish between the RAPs. This will be explained in more detail in Section II, where two alternative CM network topologies will be proposed that can be used for RoF.

Subcarrier multiplexing (SCM) [2], [7] is used on top of CM in order to serve multiple mobile terminals (MTs) simultaneously through the same RAP. This will be considered in more detail in Section III.

Finally, the performance of the proposed system will be evaluated in Section IV, illustrated by a numerical example.

Conclusions are given in Section V.

II. Coherence Multiplexing (CM)

Coherence multiplexing (CM) is a simple form of optical code division multiplexing (OCDM), in which broadband sources and delay-lines are used to multiplex signals from different users over one optical fiber cable [2]–[6]. A simple example of a CM system is depicted in Figure 2, which contains only one transmitter and receiver.

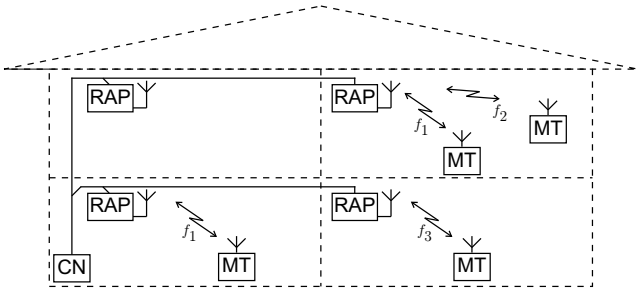

(CN=central node, RAP=radio access point, MT=mobile terminal)

Fig. 1. Example of a simple indoor Radio over Fiber network

The transmitter consists of a broadband light source and a strongly unbalanced Mach-Zehnder Interferometer (MZI). The idea is that the lightwave that passes the lower arm of the MZI is delayed with respect to the lightwave that passes the upper arm by a timeshift T_{Tx} which is much larger than the coherence time τ_{c}, such that the lightwaves do not interfere coherently, and hence, the phase modulation $\phi_{\mathrm{mod}}(t)$ does not result in a visible intensity modulation in the transmitted signal. Coherent interference can be achieved in the receiver when the path imbalance T_{Rx} in the receiver's MZI is the same as the path imbalance T_{Tx} in the transmitter's MZI. In that case, the output current of the balanced photodiode pair will contain a term that corresponds to the modulating signal $\phi_{\mathrm{mod}}(t)$. The lightwaves that interfere incoherently result into (broadband) optical beat interference (OBI) noise. When

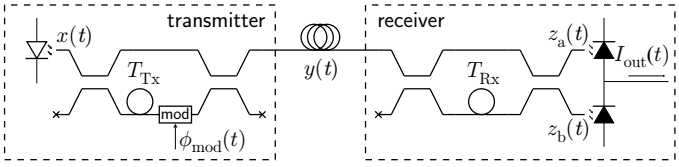

Fig. 2. A simple coherence multiplex (CM) system with one transmitter and receiver

the difference between $T_{\rm Rx}$ and $T_{\rm Tx}$ is much larger than $\tau_{\rm c}$, however, none of the lightwaves will interfere coherently; only OBI noise will result. Hence, multiplexing can be performed by assigning different delays to different users.

In this paper, CM is used as a means to distinguish between the RAPs, using a common fiber for the RF signal distribution. Several configurations are known for implementing coherence multiplexed networks [4], of which three are suitable for communications over optical fiber cables [5]. In this paper, only two of them will be considered: the parallel array and the single intrinsic reference ladder system. The third one, the discontinuous series system, can be proven not to be suitable for RoF application, because it introduces distortion in the output signal [5]. Uehara et al. [2] proposed the extrinsic reference ladder system for their RoF system using CM. This is not very practical, however, as it requires two transmission fibers. This will introduce problems, as the polarization states of the lightwaves at the outputs of these two fibers will in general not be matched.

A. The parallel array

The most straightforward network topology for CM is the parallel array. In the parallel array, each transmission node (with number i) consists of a light source with source signal $x_i(t)$ and a Mach-Zehnder Interferometer (MZI) with path-imbalance $T_{{\rm Tx},i}$ and phase modulation $\phi_{{\rm mod},i}(t)$. This is illustrated in Figure 3.

$x_i(t)$ denotes the normalized pre-envelope of the electrical field of the (linearly polarized) optical signal, in such a way that its central frequency and phase correspond to the optical frequency and phase, and the optical power coupled into the MZI follows as

$$P_{{\rm in},i}(t) = \tfrac{1}{2}\Big|x_i(t)\Big|^2 \tag{1}$$

Each source is assumed to have the same average power $P_{\rm in} = {\rm E}\big[P_{{\rm in},i}(t)\big]$. For broadband sources like LEDs or SLDs, the corresponding complex envelope can be modelled as a circular complex Gaussian process [8]. It is assumed that its power spectral density (psd) function has a Gaussian profile, such that the autocorrelation function of each $x_i(t)$ is given by

$$\begin{aligned} R_{x^*x}(\tau) &\triangleq {\rm E}\big[x_i^*(t)x_i(t+\tau)\big] \\ &= 2P_{\rm in}\exp\left(-\frac{\pi}{2}\left(\frac{\tau}{\tau_{\rm c}}\right)^2\right)\exp({\rm j}2\pi f_{\rm c}\tau) \end{aligned} \tag{2}$$

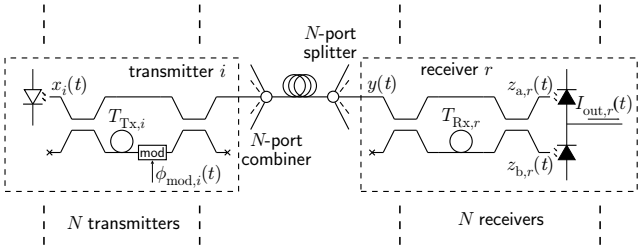

Fig. 3. The parallel array (PA)

The 2×2-couplers are uniform and have transfer matrix

$$[H_2] = \tfrac{1}{\sqrt{2}}\begin{bmatrix} 1 & {\rm j} \\ {\rm j} & 1 \end{bmatrix} \tag{3}$$

For the time being, assume that the dispersion in the fiber can be neglected. (This will be considered in Section IV.) The signal that is received by each of the (balanced) receivers can then be written as

$$y(t) = \frac{1}{2N\sqrt{L_{\rm o}}}\sum_{i=1}^{N}\Big[x_i(t) - x_i(t-T_{{\rm Tx},i})s_i(t)\Big] \tag{4}$$

where N is the number of transmission nodes, and $L_{\rm o}$ denotes the optical power loss due to propagation loss (attenuation) in the fiber, excess loss in the optical components and coupling losses in the fiber connectors. $s_i(t)$ is defined as

$$s_i(t) \triangleq \exp\Big({\rm j}\,\phi_{{\rm mod},i}(t)\Big) \tag{5}$$

The autocorrelation function of this (non-stationary) signal is given by

$$\begin{aligned} R_{y^*y}(t_1,t_2) &= {\rm E}\big[y^*(t_1)y(t_2)\big] \\ &= \frac{1}{4N^2L_{\rm o}}\sum_{i=1}^{N}\Big[R_{x^*x}(t_2-t_1) \\ &\qquad - R_{x^*x}(t_2-t_1-T_{{\rm Tx},i})s_i(t_2) \\ &\qquad - R_{x^*x}(t_2-t_1+T_{{\rm Tx},i})s_i^*(t_1) \\ &\qquad + R_{x^*x}(t_2-t_1)s_i^*(t_1)s_i(t_2)\Big] \end{aligned} \tag{6}$$

For a particular receiver r, the lightwave signals at the upper and lower output ports of the MZI can be related to the received signal $y(t)$ as

$$z_{r,{\rm a}}(t) = \tfrac{1}{2}\Big[y_L(t) - y_L(t-T_{\rm Rx})\Big] \tag{7}$$

$$z_{r,{\rm b}}(t) = \tfrac{1}{2}{\rm j}\Big[y_L(t) + y_L(t-T_{\rm Rx})\Big] \tag{8}$$

By neglecting shot noise for the time being (this will be considered in Section IV), and assuming that the photodiodes are perfectly linear with identical responsivities $R_{\rm pd}$, the instantaneous output current can be written as

$$\begin{aligned} I_{\rm out}(t) &= \tfrac{1}{2}R_{\rm pd}\Big[\big|z_{\rm a}(t)\big|^2 - \big|z_{\rm b}(t)\big|^2\Big] \\ &= -\tfrac{1}{2}R_{\rm pd}{\rm Re}\Big\{y_L(t)y_L^*(t-T_{\rm Rx})\Big\} \end{aligned} \tag{9}$$

where ${\rm Re}\{.\}$ denotes real part. This consists of (zero-mean) OBI noise and an information-carrying term. The latter can be found by taking the expected value

$${\rm E}\big[I_{{\rm out},r}(t)\big] = -\tfrac{1}{2}R_{\rm pd}{\rm Re}\Big\{R_{y^*y}(t-T_{{\rm Rx},r},t)\Big\} \tag{10}$$

Combining (2), (6) and (10), and assuming that all $T_{{\rm Tx},i}$s and $T_{{\rm Rx},r}$s are much larger than $\tau_{\rm c}$, we can write

$$\begin{aligned} &{\rm E}\big[I_{{\rm out},r}(t)\big] = \\ &\qquad \frac{R_{\rm pd}}{8N^2}\sum_{i=1}^{N}{\rm Re}\Big\{R_{x^*x}(T_{{\rm Rx},r}-T_{{\rm Tx},i})s_i(t)\Big\} \end{aligned} \tag{11}$$

Obviously, the receiver r is tuned to the corresponding transmitter r when $\left|T_{\mathrm{Rx},r} - T_{\mathrm{Tx},r}\right|$ is much smaller than τ_{c}. Crosstalk from interfering channels is avoided by spacing apart the $T_{\mathrm{Tx},i}$s much more than τ_{c}, say at least four times. Hence, a possible assignment rule is $T_{\mathrm{Tx},i} = 4i\,\tau_{\mathrm{c}}$. (11) then becomes, using (5)

$$\mathrm{E}\big[I_{\mathrm{out},r}(t)\big] = \frac{R_{\mathrm{pd}}P_{\mathrm{in}}}{4N^2}\cos\Big(2\pi f_{\mathrm{c}}(T_{\mathrm{Rx},r} - T_{\mathrm{Tx},r}) + \phi_{\mathrm{mod},r}(t)\Big) \quad (12)$$

The visibility of $\phi_{\mathrm{mod},r}(t)$ depends on the value of $2\pi f_{\mathrm{c}}(T_{\mathrm{Rx},r} - T_{\mathrm{Tx},r})$. We will come back to this in Section III.

B. The single intrinsic reference ladder (SIRL) system

The single intrinsic reference ladder (SIRL) system [5] is a specific implementation of the intrinsic reference ladder system [4]. It has one (common) light source with source signal $x(t)$ and one MZI, as illustrated in Figure 4. The 2×2-couplers of the MZI are non-uniform with power coupling factor κ, so they have transfer matrix

$$[H_2] = \begin{bmatrix} \sqrt{\kappa} & \mathrm{j}\sqrt{1-\kappa} \\ \mathrm{j}\sqrt{1-\kappa} & \sqrt{\kappa} \end{bmatrix} \quad (13)$$

The lower arm of the MZI is subdivided in N sub-branches, each subbranch containing a delay $T_{\mathrm{Tx},i}$ with respect to the upper (reference) arm and a phase modulation $\phi_{\mathrm{mod},i}(t)$. The signal that is received by each of the receivers can now be written as

$$y(t) = \frac{\kappa}{\sqrt{N\,L_{\mathrm{o}}}}x(t) - \frac{1-\kappa}{N\sqrt{N\,L_{\mathrm{o}}}}\sum_{i=1}^{N} x(t - T_{\mathrm{Tx},i})s_i(t) \quad (14)$$

which has autocorrelation function

$$\begin{aligned} R_{y^*y}(t_1,t_2) &= \frac{\kappa^2}{N\,L_{\mathrm{o}}}R_{x^*x}(t_2 - t_1) \\ &- \frac{\kappa(1-\kappa)}{N^2\,L_{\mathrm{o}}}\sum_{i=1}^{N}\Big[R_{x^*x}(t_2 - t_1 - T_{\mathrm{Tx},i})s_i(t_2) \\ &\qquad + R_{x^*x}(t_2 - t_1 + T_{\mathrm{Tx},i})s_i^*(t_1)\Big] \\ &+ \frac{(1-\kappa)^2}{N^3\,L_{\mathrm{o}}}\sum_{i=1}^{N}\sum_{j=1}^{N} R_{x^*x}(t_2 - t_1 + T_{\mathrm{Tx},i} - T_{\mathrm{Tx},j}) \\ &\qquad \cdot s_i^*(t_1)s_j(t_2) \end{aligned} \quad (15)$$

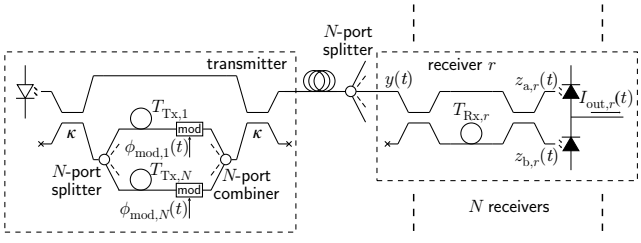

Fig. 4. The single intrinsic reference ladder system (SIRL)

Using (10), the output signal of receiver r now follows as

$$\begin{aligned} &\mathrm{E}\big[I_{\mathrm{out},r}(t)\big] = \\ &\frac{R_{\mathrm{pd}}\kappa(1-\kappa)}{2N^2\,L_{\mathrm{o}}}\sum_{i=1}^{N}\mathrm{Re}\Big\{R_{x^*x}(T_{\mathrm{Rx},r} - T_{\mathrm{Tx},i})s_i(t)\Big\} \\ &- \frac{R_{\mathrm{pd}}(1-\kappa)^2}{2N^3\,L_{\mathrm{o}}}\sum_{i=1}^{N}\sum_{j=1}^{N}\mathrm{Re}\Big\{R_{x^*x}(T_{\mathrm{Rx},r} + T_{\mathrm{Tx},i} - T_{\mathrm{Tx},j}) \\ &\qquad \cdot s_i(t - T_{\mathrm{Rx},r})s_j(t)\Big\} \end{aligned} \quad (16)$$

Obviously, the receiver r is again tuned to the corresponding transmitter r when $\left|T_{\mathrm{Rx},r} - T_{\mathrm{Tx},r}\right|$ is much smaller than τ_{c}. Crosstalk from interfering channels is avoided by spacing apart the $T_{\mathrm{Tx},i}$s much more than τ_{c} (say at least four times), and moreover, $\left|T_{\mathrm{Rx},r} + T_{\mathrm{Tx},i} - T_{\mathrm{Tx},j}\right|$ should also be much larger than τ_{c} for any values of i, j and r. Hence, a possible assignment rule is $T_{\mathrm{Tx},i} = 4(2i-1)\tau_{\mathrm{c}}$. (16) then becomes

$$\begin{aligned} \mathrm{E}\big[I_{\mathrm{out},r}(t)\big] &= \frac{R_{\mathrm{pd}}P_{\mathrm{in}}\kappa(1-\kappa)}{N^2\,L_{\mathrm{o}}} \\ &\cdot \cos\Big(2\pi f_{\mathrm{c}}(T_{\mathrm{Rx},r} - T_{\mathrm{Tx},r}) + \phi_{\mathrm{mod},r}(t)\Big) \end{aligned} \quad (17)$$

Note that this result is similar to (12). (For $\kappa = \frac{1}{2}$ and $N = 1$ they are exactly the same, as expected.)

The main difference between the parallel array and the SIRL system is that in the SIRL system, the transmitters are localized to a single node. Therefore, the SIRL system cannot be applied in the upstream direction of the distribution network. An advantage of the SIRL system, however, is that it requires only one light source rather than N light sources. The performances of the two alternatives will be compared in Section IV.

III. Subcarrier Multiplexing (SCM)

In order to serve multiple (say K) mobile terminals simultaneously through the same RAP, subcarrier multiplexing (SCM) is performed on each CM channel. This means that for each transmitter i, the modulating signal $\phi_{\mathrm{mod},i}(t)$ is in fact a composite signal consisting of K subcarrier channels. If the subcarrier channels are multiplexed using frequency division multiplexing (FDM), then the composite signal can be written as

$$\phi_{\mathrm{mod},i}(t) = \sum_{k=1}^{K}\beta_{i,k}(t)\cos\Big(2\pi f_k t + \psi_{i,k}(t)\Big) \quad (18)$$

where $\beta_{i,k}(t)$ is the amplitude, f_k is the carrier frequency and $\psi_{i,k}(t)$ is the phase of the k-th subcarrier channel of the i-the RAP. In general, f_k will be in the RF-regime, and $\beta_{i,k}(t)$ and/or $\psi_{i,k}(t)$ are modulated by the information signal, depending on the modulation format that is to be used for the mobile channel (for example QAM).

For the parallel array, this will result in an output signal

$$\begin{aligned}\mathrm{E}\big[I_{\mathrm{out},r}(t)\big] =& \\ \frac{R_{\mathrm{pd}}P_{\mathrm{in}}}{4N^2L_{\mathrm{o}}}\Bigg[&\cos\Big(2\pi f_{\mathrm{c}}(T_{\mathrm{Rx},r}-T_{\mathrm{Tx},r})\Big)\\ &\cdot\cos\left(\sum_{k=1}^{K}\beta_{r,k}(t)\cos\Big(2\pi f_k t+\psi_{r,k}(t)\Big)\right)\\ &-\sin\Big(2\pi f_{\mathrm{c}}(T_{\mathrm{Rx},r}-T_{\mathrm{Tx},r})\Big)\\ &\cdot\sin\left(\sum_{k=1}^{K}\beta_{r,k}(t)\cos\Big(2\pi f_k t+\psi_{r,k}(t)\Big)\right)\Bigg] \quad (19)\end{aligned}$$

Obviously, the relation between the output signal and the subcarrier channels is non-linear. As a result, intermodulation (IMD) between the subcarrier channels will occur. This will be further quantified in Subsection IV-C. For the time being, however, we will assume that $K\cdot\beta_{r,k}$ is much smaller than $\frac{\pi}{2}$, such that we can approximate the output signal by its first order Taylor expansion

$$\begin{aligned}\mathrm{E}\big[I_{\mathrm{out},r}(t)\big] \approx& \\ \frac{R_{\mathrm{pd}}P_{\mathrm{in}}}{4N^2L_{\mathrm{o}}}\Bigg[&\cos\Big(2\pi f_{\mathrm{c}}(T_{\mathrm{Rx},r}-T_{\mathrm{Tx},r})\Big)\\ &-\sin\Big(2\pi f_{\mathrm{c}}(T_{\mathrm{Rx},r}-T_{\mathrm{Tx},r})\Big)\\ &\cdot\left(\sum_{k=1}^{K}\beta_{r,k}(t)\cos\Big(2\pi f_k t+\psi_{r,k}(t)\Big)\right)\Bigg] \quad (20)\end{aligned}$$

Apparently, the signal can be approximated by a DC-term plus the SCM channels. The amplitudes of the SCM channels in the output signal can be optimized by for example choosing

$$2\pi f_{\mathrm{c}}(T_{\mathrm{Rx},r}-T_{\mathrm{Tx},r})=\tfrac{3\pi}{2} \quad (21)$$

The DC-term then disappears, such that the output signal becomes

$$\begin{aligned}\mathrm{E}\big[I_{\mathrm{out},r}(t)\big] \approx& \\ &\frac{R_{\mathrm{pd}}P_{\mathrm{in}}}{4N^2L_{\mathrm{o}}}\sum_{k=1}^{K}\beta_{r,k}(t)\cos\Big(2\pi f_k t+\psi_{r,k}(t)\Big) \quad (22)\end{aligned}$$

Note that this requires active control, as the value of $2\pi f_{\mathrm{c}}(T_{\mathrm{Rx},r}-T_{\mathrm{Tx},r})$ is very sensitive for changes in temperature in either the transmitter or receiver. This can be done by detecting the DC-term in (20) using a low-pass filter, and aplying a feedback loop that increases the value of $T_{\mathrm{Rx},r}$ when this DC-term is positive, and vice-versa.

IV. Performance analysis

Let us now assess the feasibility of the proposed RoF distribution network by analyzing the performance of a particular configuration. We will start by giving a description of this particular configuration, and then analyze the effects of chromatic dispersion and losses in the fibers, intermodulation distortion (IMD) between the SCM channels, optical beat interference (OBI) noise, shot noise and thermal noise. Note that the analysis will be focussed on the optical transport part of the network, hence not incorporating the wireless transmission path.

A. Configuration

An RoF distribution network is considered for transporting wireless local area network (WLAN) signals. In particular, we will consider the 11 Mbps version of IEEE 802.11b [9]. Using the European frequency set 1, it has $K=3$ carriers, at $f_1=2412$ MHz, $f_2=2442$ MHz and $f_3=2472$ MHz. CCK modulation is used, resulting in constant SCM channel amplitudes

$$\beta_{r,k}(t)=\beta \quad (23)$$

and effective channel bandwidths $W\approx 17$ MHz.

For the transmission medium, standard single mode fiber (SMF) [10] of 500 m length (a typical indoor length) is assumed. It will be shown that it has to be operated in close proximity to the zero-dispersion wavelength (1310 nm) in order to limit the effect of dispersion.

The coherence time τ_{c} of the optical sources will be assumed to be 0.1 ps. (At 1310 nm, this corresponds to a linewidth of approximately 40 nm.) The reason for choosing such a low coherence time is to keep the length of the delay lines in the optical circuits within reasonable bounds and moreover, to minimize the effect of OBI noise. The latter will become clear in Subsection IV-D. The power that is launched into the fiber is assumed to be $P_{\mathrm{in}}=10$ mW. The responsivities R_{pd} of the photodiodes are assumed to be 0.8 A/W.

B. Chromatic dispersion and losses

So far, chromatic dispersion in the single-mode fibers (SMFs) has been ignored in the analysis of the system. Since, broadband sources are used, however, the effect of dispersion cannot be neglected. The effect of dispersion in a single-mode CM system has been analyzed in [6], resulting in the impulse response of a one transmitter system. For this application, however, it is more convenient to work with the transfer function, which can be found by Fourier transforming the impulse response in [6], resulting in

$$\begin{aligned}H_{\mathrm{sys}}(f) =& \\ &\frac{R_{\mathrm{pd}}P_{\mathrm{in}}}{4L_{\mathrm{o}}}\frac{\exp\left(-\dfrac{\pi f^2T_1^2}{1+\mathrm{j}fT_2/2}\right)}{\sqrt{1+\mathrm{j}fT_2/2}}\exp(-\mathrm{j}2\pi f\,T_0) \quad (24)\end{aligned}$$

where

$$T_0 = L\,\tau_{\mathrm{g}}(\lambda_{\mathrm{c}}) \quad (25)$$

$$T_1 = -\frac{L\,\lambda_{\mathrm{c}}^2\tau_{\mathrm{g}}'(\lambda_{\mathrm{c}})}{\sqrt{2}\tau_{\mathrm{c}}c_0} \quad (26)$$

$$T_2 = \frac{L\,\lambda_{\mathrm{c}}^3}{\tau_{\mathrm{c}}^2c_0^2}\Big[2\tau_{\mathrm{g}}'(\lambda_{\mathrm{c}})+\lambda_{\mathrm{c}}\tau_{\mathrm{g}}''(\lambda_{\mathrm{c}})\Big] \quad (27)$$

L is the length of the fiber, $\tau_{\rm g}(\lambda_{\rm c})$ is the group delay per unit length as a function of center wavelength $\lambda_{\rm c}$ and c_0 is the speed of light in vacuum. $\tau'_{\rm g}(\lambda_{\rm c})$ and $\tau''_{\rm g}(\lambda_{\rm c})$ are the first and second derivative of $\tau_{\rm g}$ with respect to wavelength, evaluated at the center wavelength $\lambda_{\rm c}$; these are also known as the first and second order dispersion coefficients, respectively.

Let's consider standard SMF [10] at a typical indoor length of 500 m, with center wavelengths of 1550 nm and 1310 nm, and a coherence time of 0.1 ps.

1) 1550 nm: this is a common wavelength in fiber optics, as it corresponds to the amplification window of erbium-doped fiber amplifiers (EDFAs). At this wavelength, second order dispersion can be neglected ($T_2 \ll T_1$), and the prescribed value for the first order dispersion coefficient is $\tau'_{\rm g}(\lambda_{\rm c}) < 20$ ps/(nm·km) [10]. Using (26), we find $T_1 \approx 566$ ps. Calculating the absolute value of (24), we find a dispersion-induced penalty of the signal amplitude at 2.4 GHz of approximately 50 dB. Hence, a center wavelength 1550 nm is certainly not suitable for this application with standard SMF.

2) 1310 nm: at this wavelength, there is no first order dispersion, so $T_1 = 0$. The prescribed value for the second order dispersion coefficient is $\tau''_{\rm g}(\lambda_{\rm c}) < 0.093$ ps/(nm^2·km) [10]. Using (27), we find $T_2 = 152$ ps, resulting in a dispersion-induced penalty of the signal amplitude at 2.4 GHz of approximately 0.07 dB, which can be neglected. It can be verified (by analyzing the magnitude and phase of (24) around $f = 2.4$ GHz) that magnitude and phase distortion can also be neglected.

The loss $L_{\rm o}$ comprises propagation losses, excess losses in components and coupling losses in fiber-chip connections. Assuming a fiber attenuation loss at 1310 nm of 0.35 dB/km, an excess loss of approximately 0.2 dB per MZI, an excess loss of approximately 0.5 dB per coupler or combiner and a coupling loss of approximately 0.3 dB per fiber-chip coupling, we find $L_{\rm o} \approx 2.03$ (3.1 dB).

C. Intermodulation distortion (IMD)

The relation between the expected output signal of the CM receiver and the modulating signal in the CM transmitter is non-linear, as can be seen from (19). Hence, intermodulation distortion (IMD) between the SCM channels will occur [2], [7]. This can be quantified by substituting (21) and (23) into (19) and making a third order Taylor expansion

$$\begin{aligned}\mathrm{E}\big[I_{{\rm out},r}(t)\big] &= \frac{R_{\rm pd}P_{\rm in}}{4N^2L_{\rm o}}\sin\left(\beta\sum_{k=1}^{3}\cos\Big(2\pi f_k t+\psi_{r,k}(t)\Big)\right)\\ &\approx \frac{R_{\rm pd}P_{\rm in}}{4N^2L_{\rm o}}\left[\beta\sum_{k=1}^{3}\cos\Big(2\pi f_k t+\psi_{r,k}(t)\Big)\right.\\ &\qquad\left.-\tfrac{1}{6}\left(\beta\sum_{k=1}^{3}\cos\Big(2\pi f_k t+\psi_{r,k}(t)\Big)\right)^3\right] \quad (28)\end{aligned}$$

Expanding the third-order term results into $4K^3 = 108$ sinusoidal terms, each with amplitude

$$\frac{R_{\rm pd}P_{\rm in}}{4N^2L_{\rm o}}\cdot\frac{\beta^3}{24}$$

and frequencies $\big|f_l \pm f_m \pm f_n\big|$, where f_l, f_m and f_n can take any of the SCM channel frequencies.

It can be shown that 45 of these terms contribute equally to the three desired channels. Together with the first order terms, this result in a third-order approximation of the amplitude per channel that is given by

$$A_{\rm c} \approx \frac{R_{\rm pd}P_{\rm in}}{4N^2L_{\rm o}}\left(\beta-\tfrac{5}{8}\beta^3\right) \quad (29)$$

The terms with the following frequency contribute to third order IMD:

- $f_2+f_2-f_3 = 2412$ MHz $= f_1$ (3 terms)
- $f_1-f_2+f_3 = 2442$ MHz $= f_2$ (6 terms)
- $f_2+f_2-f_1 = 2472$ MHz $= f_3$ (3 terms)

(The other terms do not coincide with the SCM channels.) Hence, the most IMD occurs in the second SCM channel; it has amplitude

$$\sigma_{\rm IMD} = \frac{R_{\rm pd}P_{\rm in}}{4N^2L_{\rm o}}\cdot\frac{\beta^3}{4} \quad (30)$$

Note, however, that the third-order IMD products do not have the same spectral shape as the SCM channels themselves, as these IMD products are broadened because of three-fold mixing. By making the simplifying assumption that the spectral shape of an SCM channel is roughly rectangular, it can be derived by three-fold convolution that the spectrum of the third-order IMD products is roughly piecewise parabolic. Integration then shows that $\frac{2}{3}$ of its area coincides with the rectangular spectrum of the SCM channel. Hence, the signal-to-IMD ratio for the second SCM channel is roughly

$$CIR_{\rm IMD} \approx \tfrac{3}{2}\left(\frac{A_{\rm c}}{\sigma_{\rm IMD}}\right)^2 = 24\left(\frac{1}{\beta^2}-\tfrac{5}{8}\right)^2 \quad (31)$$

It can be easily proven that this equation holds for both the parallel array and the SIRL system.

D. Optical beat interference (OBI) noise

Optical beat interference (OBI) noise results from mixing of mutually incoherent lightwaves. Its power spectral density can be found by Fourier transforming the covariance function of (9). Using the fourth-order moment theorem for circular Gaussian variables [8], it can be proven that the latter is given by

$$\begin{aligned}C_{I_{\rm out}}(t_1,t_2) &\triangleq \mathrm{E}\big[I_{\rm out}(t_1)I_{\rm out}(t_2)\big]\\ &\qquad -\mathrm{E}\big[I_{\rm out}(t_1)\big]\mathrm{E}\big[I_{\rm out}(t_2)\big]\\ &= \tfrac{1}{8}R_{\rm pd}^2\mathrm{Re}\Big\{R_{y^*y}(t_1,t_2)R_{y^*y}(t_2-T_{{\rm Rx},r},t_1-T_{{\rm Rx},r})\\ &\qquad +R_{y^*y}(t_1,t_2-T_{{\rm Rx},r})R_{y^*y}(t_2,t_1-T_{{\rm Rx},r})\Big\} \quad (32)\end{aligned}$$

For the parallel array, this can be evaluated using (6). Taking into account the predefined conditions for the delays, this can

be proven to result in

$$C_{I_{\rm out}}(t_1,t_2) = \frac{R_{\rm pd}^2}{128N^4L_{\rm o}^2}{\rm Re}\Bigg\{\Big|R_{x^*x}(t_2-t_1)\Big|^2 \cdot\sum_{i=1}^{N}\sum_{j=1}^{N}\Big[1+s_i^*(t_1)s_i(t_2)\Big]\Big[1+s_j^*(t_1)s_j(t_2)\Big] + \sum_{i=1}^{N}\Big[R_{x^*x}(t_2-t_1+T_{{\rm Tx},i})s_i^*(t_2) \cdot R_{x^*x}(t_1-t_2-T_{{\rm Tx},i})s_i(t_1-T_{{\rm Rx},r}) + R_{x^*x}(t_2-t_1-T_{{\rm Tx},i})s_i(t_1) \cdot R_{x^*x}(t_1-t_2+T_{{\rm Tx},i})s_i^*(t_2-T_{{\rm Rx},r})\Big] + R_{x^*x}(t_2-t_1-T_{{\rm Rx},r}+T_{{\rm Tx},r})s_r^*(t_1) \cdot R_{x^*x}(t_1-t_2-T_{{\rm Rx},r}+T_{{\rm Tx},r})s_r^*(t_2)\Bigg\} \quad (33)$$

Using (2), (18) and (21) and assuming that

- $\big|T_{{\rm Rx},r}-T_{{\rm Tx},r}\big|$ is much smaller than $\tau_{\rm c}$,
- both the carrier frequencies and the bandwidths of the SCM channels are much smaller than the inverse of any delay,
- β is much smaller than $\frac{\pi}{2}$,

it can be proven that this reduces to

$$C_{I_{\rm out}}(t_1,t_2) \approx \frac{R_{\rm pd}^2}{128N^4L_{\rm o}^2}\Bigg\{(4N^2-1)\Big|R_{x^*x}(t_2-t_1)\Big|^2 + \sum_{i=1}^{N}\Bigg[\Big|R_{x^*x}(t_2-t_1+T_{{\rm Tx},i})\Big|^2 + \Big|R_{x^*x}(t_2-t_1-T_{{\rm Tx},i})\Big|\Bigg]\Bigg\} \quad (34)$$

Hence, the OBI noise $I_{\rm bn}(t)$ can be considered as wide-sense stationary. As a result, we can calculate its power spectral density function, by using (2) and Fourier transforming (34) with respect to t_1-t_2, resulting in

$$S_{I_{\rm bn}}(f) \approx \frac{R_{\rm pd}^2P_{\rm in}^2\tau_{\rm c}}{32N^4L_{\rm o}^2}\exp\big(-\pi(f\,\tau_{\rm c})^2\big) \cdot\left(4N^2-1+2\sum_{i=1}^{N}\cos(2\pi f T_{{\rm Tx},i})\right) \quad (35)$$

As both the carrier frequencies and the bandwidths of the SCM channels are much smaller than the inverse of both $\tau_{\rm c}$ and $T_{{\rm Tx},i}$, we can simply consider the OBI noise as additive white Gaussian noise with power spectral density

$$S_{I_{\rm bn}}(0) \approx \frac{R_{\rm pd}^2P_{\rm in}^2\tau_{\rm c}}{32N^4L_{\rm o}^2}(4N^2+2N-1) \quad (36)$$

Consequently, the carrier-to-OBI noise ratio for one SCM channel, using the parallel array, is

$$CNR_{\rm bn} \triangleq \frac{\frac{1}{2}A_{\rm c}^2}{2S_{I_{\rm bn}}(0)W} \approx \frac{\big(\beta-\frac{5}{8}\beta^3\big)^2}{2(4N^2+2N-1)W\tau_{\rm c}} \quad (37)$$

A similar analysis can be performed for the SIRL system, using (15), which results in

$$CNR_{\rm bn} \approx \frac{\big(\beta-\frac{5}{8}\beta^3\big)^2}{2\left[\frac{\kappa^2N^2}{(1-\kappa)^2}+4N-1+\frac{(1-\kappa)^2(2N-1)}{\kappa^2N}\right]W\tau_{\rm c}} \quad (38)$$

E. Shot noise

Shot noise arises as a result of the random arrival times of photons in the photodiodes. It can be considered as white noise, with a power spectral density $S_{I_{\rm sn}}(f)$ that can be found using Schottky's formula. As the shot noise currents in the photodiodes are mutually independent, this results in

$$S_{I_{\rm sn}}(f) = \tfrac{1}{2}e\,R_{\rm pd}\left[\big|z_a(t)\big|^2+\big|z_b(t)\big|^2\right] = \tfrac{1}{4}e\,R_{\rm pd}\left[\big|y(t)\big|^2+\big|y(t-T_{{\rm Rx},r})\big|^2\right] \quad (39)$$

where $e=1.6\cdot10^{-19}$ C is the charge of an electron. For the parallel array, this can be evaluated using (2) and (6), resulting in

$$S_{I_{\rm sn}}(f) = \frac{e\,R_{\rm pd}P_{\rm in}}{2N\,L_{\rm o}} \quad (40)$$

so the carrier-to-shot noise ratio of the parallel array is given by

$$CNR_{\rm sn} \triangleq \frac{\frac{1}{2}A_{\rm c}^2}{2S_{I_{\rm sn}}(0)W} = \frac{R_{\rm pd}P_{\rm in}\big(\beta-\frac{5}{8}\beta^3\big)^2}{32N^3L_{\rm o}\,W\,e} \quad (41)$$

and for the SIRL system, one can use (15), resulting in

$$S_{I_{\rm sn}}(f) = \frac{e\,R_{\rm pd}P_{\rm in}}{N\,L_{\rm o}}\left[\kappa^2N+(1-\kappa)^2\right] \quad (42)$$

and

$$CNR_{\rm sn} = \frac{R_{\rm pd}P_{\rm in}\big(\beta-\frac{5}{8}\beta^3\big)^2}{4N^2\left[\frac{N}{(1-\kappa)^2}+\frac{1}{\kappa^2}\right]L_{\rm o}\,W\,e} \quad (43)$$

F. Thermal noise

Thermal noise results from the random motion of charge carriers in resistive parts of the receiver's electronics. Assuming a load resistor $R_{\rm L}=50\ \Omega$ with temperature $T_{\rm R}=300$ K and a pre-amplifier noise figure $F_{\rm n}=2.40$ (3.8 dB), we can find for the power spectral density of the equivalent input noise current $I_{\rm tn}(t)$ of the amplifier:

$$S_{I_{\rm tn}}(f) = \frac{2k_{\rm B}T_{\rm R}F_{\rm n}}{R_{\rm L}} \quad (44)$$

where $k_{\rm B}=1.38\cdot10^{-38}$ is Boltzmann's constant. Hence, we find for carrier-to-thermal noise ratio for the parallel array

$$CNR_{\rm tn} \triangleq \frac{\frac{1}{2}A_{\rm c}^2}{2S_{I_{\rm tn}}(0)W} = \frac{R_{\rm pd}^2P_{\rm in}^2\big(\beta-\frac{5}{8}\beta^3\big)^2R_{\rm L}}{128N^4L_{\rm o}^2W\,k_{\rm B}T_{\rm R}F_{\rm n}} \quad (45)$$

and for the SIRL system

$$CNR_{\rm tn} = \frac{R_{\rm pd}^2P_{\rm in}^2\big(\beta-\frac{5}{8}\beta^3\big)^2R_{\rm L}\kappa^2(1-\kappa)^2}{8N^4L_{\rm o}^2W\,k_{\rm B}T_{\rm R}F_{\rm n}} \quad (46)$$

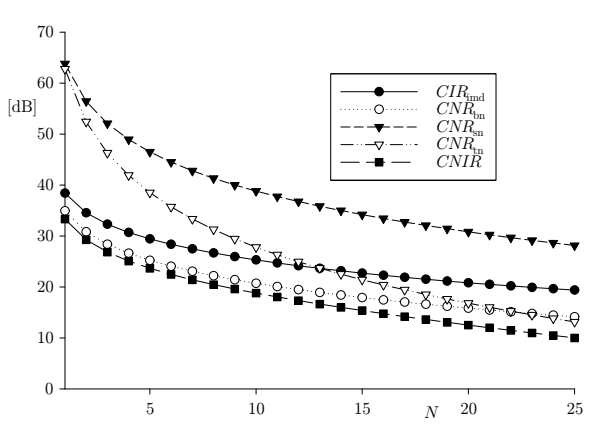

(a) Maximum CNIR for the parallel array

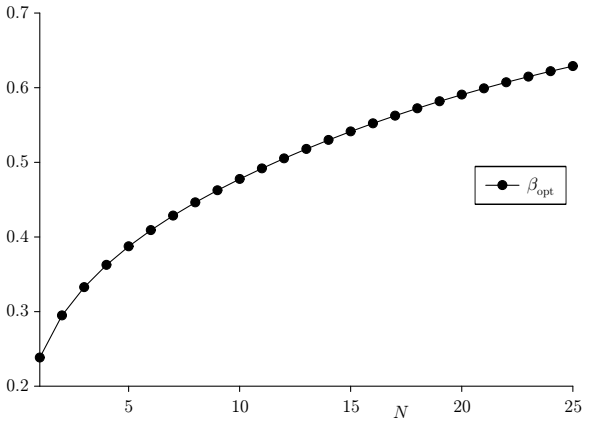

(b) Optimum modulation index β for the parallel array

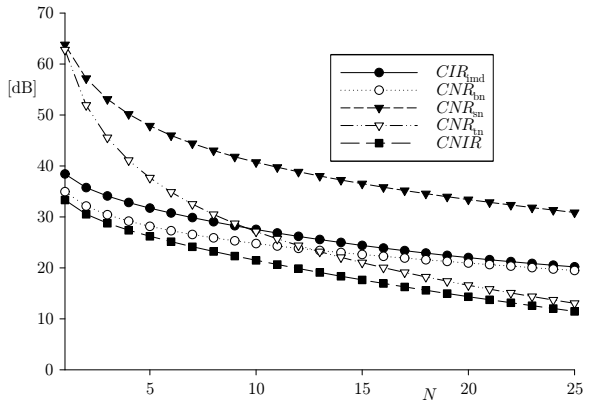

(c) Maximum CNIR for the SIRL system with $\kappa = \frac{1}{2}$

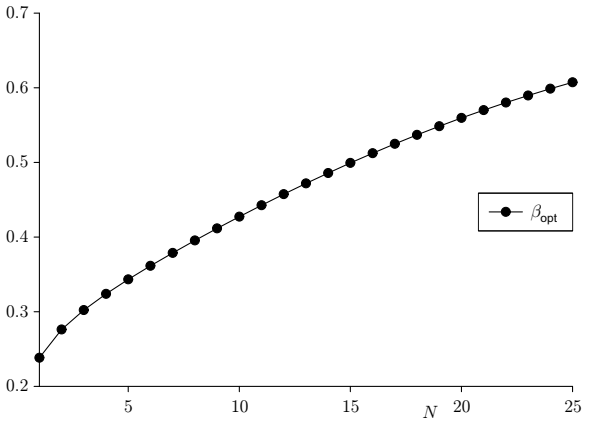

(d) Optimum modulation index β for the SIRL system with $\kappa = \frac{1}{2}$

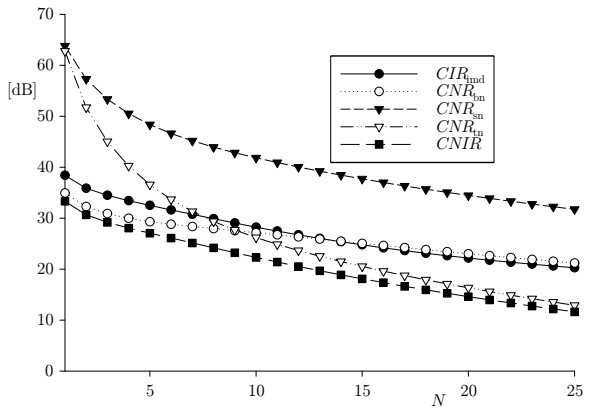

(e) Maximum CNIR for the SIRL system with optimized κ

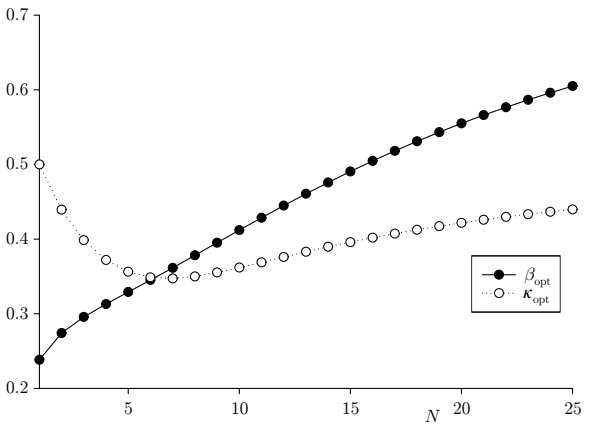

(f) Optimum modulation index β and coupling coefficient κ for the SIRL system

Fig. 5. Maximum CNIR and optimum values of modulation index β and coupling coefficient κ as a function of number of RAPs N

G. Overall performance

The overall performance of the parallel array and SIRL system can be expressed as the carrier-to-noise and intermodulation ratio. It can be calculated by

$$CNIR^{-1} = CIR_{\mathrm{IMD}}^{-1} + CNR_{\mathrm{bn}}^{-1} + CNR_{\mathrm{sn}}^{-1} + CNR_{\mathrm{tn}}^{-1} \quad (47)$$

For the parallel array, this results in an expression that depends on the modulation index β. Numerical optimization provides numerical values for the maximum CNIR that are given in Figure 5(a), and optimum values for β that are given in Figure 5(b).

In case of the SIRL system, the CNIR depends on β, and also on the coupling coefficient κ of the 2×2-couplers in the

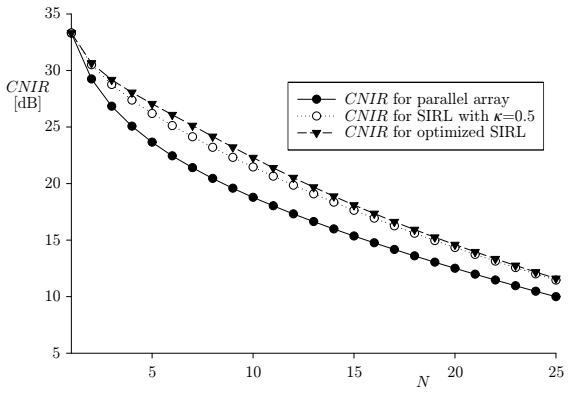

Fig. 6. Maximum CNIR for the parallel array, the SIRL system with $\kappa = \frac{1}{2}$ and the optimized SIRL system, as a function of the number of RAPs N

transmitters' MZIs. In case of uniform couplers, we have $\kappa = \frac{1}{2}$; numerically optimizing the CNIR with respect to β then gives the results in Figure 5(c) and 5(d). When optimization is performed with respect to κ as well, however, we get the results in Figure 5(e) and 5(f).

Care must be taken when interpreting the results. It can be verified that the third-order approximation of $\sin(x)$ is reasonably accurate when $x \leq \frac{\pi}{2}$. Hence, the third-order approximation in (28) only holds for $\beta \leq \frac{\pi}{6} \approx 0.52$. As a result, the accuracy of the CNIRs that were derived can only be guaranteed for $N \leq 13$ for the parallel array, $N \leq 16$ for the SIRL system with $\kappa = \frac{1}{2}$ and $N \leq 17$ for the optimized SIRL system.

In order to compare the results, the overall CNIRs of the three system alternatives are plotted together in Figure 6. Obviously, the SIRL system performs significantly better than the parallel array: up to a few dB for values of N around 10. The difference between the SIRL system with $\kappa = \frac{1}{2}$ and the SIRL system with optimized κ is quite small, however, so it appears that for this configuration, it does not make much sense to precisely optimize the coupling coefficient κ.

The computed CNIRs apply to the signals that are fed to the antennas in the RAPs. The CNIR at the MTs should be in the order of 7.5 dB in order to keep the packet error rate (PER) below 10%. Allowing the optical distribution network to introduce a small penalty of 0.5 dB in the link budget, it can be shown that the CNIR of the antenna signal should be approximately 17 dB. Putting this as a criterium, it appears that the distribution network can achieve a satisfying performance with up to 12 RAPs using the parallel array, and with up 16 RAPs using the (optimized) SIRL system.

V. Conclusion

An RoF system was proposed for distributing RF signals to the RAPs over SMF, using a combination of CM and SCM. As two alternative CM network topologies, the parallel array and SIRL system were proposed. SCM is based on FDM. Analysis (incorporating the effect of fiber dispersion, losses, IMD, OBI noise, shot noise and thermal noise) has shown that application of such a system for serving three 11 Mbps WLAN users per RAP should be feasible, up to approximately 12 RAPs using the parallel array and up to 16 using the SIRL system, at a minimum CNIR for the antenna signal of 17 dB. The SIRL can only be used for the downlink, however.

Acknowledgment

A. Meijerink would like to thank Philips Research for funding his Ph.D. position.

References

[1] H. Al-Raweshidy (ed.), S. Komaki (ed.), *Radio over Fiber Technology*, Artech House, 2002.

[2] H. Uehara, I. Sasase, "Coherence Multiplexed/Subcarrier Multiplexing (CM/SCM) Lightwave System for Microcellular Mobile Communications", *IEICE Trans. Commun.*, Vol. E79-B, No. 5, pp. 708–715, 1996.

[3] G.J. Pendock, D.D. Sampson, "Capacity of coherence-multiplexed CDMA networks", *Opt. Commun.*, vol. 143, pp. 109–117, 1997.

[4] J.L. Brooks, R.H. Wentworth, R.C. Youngquist, M. Tur, B.Y. Kim, H.J. Shaw, "Coherence Multiplexing of Fiber-Optic Interferometric Sensors", *J. Lightwave Technol.*, Vol. 3, No. 5, pp. 1062-1072, 1985.

[5] A. Meijerink, R.O. Taniman, W. van Etten, "Comparison of three coherence multiplex system topologies", *Proc. 7^{th} Ann. Symp. IEEE/LEOS Benelux Chapt.*, Enschede, The Netherlands, 2003, to be published.

[6] A. Meijerink, N. Niëns, G.H.L.M. Heideman, W. van Etten, "Chromatic fiber dispersion in single-mode coherence multiplex systems and its impact on digital transmission", *Proc. 10^{th} Symposium on Communications and Vehicular Technology in the Benelux*, Eindhoven, The Netherlands, 2003.

[7] R. Gross, R. Olshansky, "Third-Order Intermodulation Distortion in Coherent Subcarrier-Multiplexed Systems", *IEEE Photon. Technol. Lett.*, Vol. 1, No. 8, pp. 91–93, 1989.

[8] J.W. Goodman, *Statistical Optics*, Wiley, New York, 1985.

[9] *IEEE 802.11b-1999 Supplement to 802.11-1999,Wireless LAN MAC and PHY specifications: Higher speed Physical Layer (PHY) extension in the 2.4 GHz band*, `http://standards.ieee.org/getieee802/802.11.html`, The Institute of Electrical and Electronics Engineers, 2000.

[10] *Characteristics of a single-mode optical fibre cable*, ITU-T Recommendation G.652, International Telecommunication Union, 1993.